

Experimental and computational investigations of a Cadmium(II) mononuclear complex with 2,6-Bis(3,5-dimethyl-N-pyrazolyl)pyridine (bdmpp) and selenocyanate as ligands

Research Article

Sinem Odabaşıoğlu^a, Raif Kurtaran^{a,*}, Akin Azizoglu^a, Hülya Kara^b, Sevi Öz^c, Orhan Atakol^c

^aDepartment of Chemistry, Faculty of Arts and Sciences, Balıkesir University, Cagis 10145, Balıkesir, Turkey

^bDepartment of Physics, Faculty of Arts and Sciences, Balıkesir University, Cagis 10145, Balıkesir, Turkey

^cDepartment of Chemistry, Faculty of Sciences, University of Ankara, Tandoğan, 06100, Ankara, Turkey

Received 26 September 2008; Accepted 21 December 2008

Abstract: A new cadmium (II) complex, $[\text{Cd}(\text{bdmpp})(\text{SeCN})_2(\text{H}_2\text{O})]$ (**1**) (where bdmpp = 2,6-bis(3,5-dimethyl-N-pyrazolyl)pyridine), has been synthesized and characterized by elemental and spectral (IR, ¹H-NMR and ¹³C-NMR, UV-Vis) analyses, differential scanning calorimetry, and single crystal X-ray diffraction studies. X-ray analysis showed that the structure was crystallized in the monoclinic space group Cc with a = 9.031(2), b = 13.884(3), c = 16.910(3) Å, and Z = 4. The geometry around the cadmium atom is distorted octahedral with a CdN₃Se₂O setup. The N atoms of the SeCN are engaged in two strong intermolecular H-bonding interactions forming a 3D supramolecular polymeric network. The geometry and vibrational frequencies of complex **1** computed with the DFT methods (BLYP, B3LYP, B3PW91, MPW1PW91) are in better agreement with experiment than those obtained with the ab-initio method except for the bond angles. The molecular orbital diagram has been also calculated and visualized at the B3LYP/LanL2DZ level of theory.

Keywords: Pyrazolyl complexes • Selenocyanate • Octahedral geometry Cd(II) complexes • Thermal analysis • DFT, ab-initio • NMR analysis, chirality

© Versita Warsaw and Springer-Verlag Berlin Heidelberg.

1. Introduction

The compound 2,6-bis(3,5-dimethyl-N-pyrazolyl)pyridine (bdmpp) [1] has been used as versatile terpyridine analogue ligand because of its easy preparation and modification to prepare copper [2], cobalt [3] and mercury [4] monomeric complexes, and nickel [5] and cadmium [6] dinuclear complexes with the aid of pseudohalogen. Transition metal complexes with pseudohalogen have attracted much interest due to their structures and

magnetic properties [7-9]. While charged ligands like azide and thiocyanate, however, are known for their versatile behaviors as bridging ligands in end-to-end and/or end-on fashions [10,11], complexes containing selenocyanate anion have been rarely studied so far. The selenocyanate ligand is a versatile ligand which can act as a monodentate [2] as well as a bridging group adopting the end-on $\mu(1,1)$ and end-to-end $\mu(1,3)$ bridging modes. Both possibilities have been structurally well characterized for transition metal complexes [11].

* E-mail: kurtaran@balikesir.edu.tr

We have previously described the crystal structures, spectroscopic and thermal analysis of $[\text{Cu}(\text{bdmpp})(\text{SeCN})_2]$ [2]. In this study, as a part of our ongoing research on the synthesis and structural characterization of complexes with pseudohalide ligand, the synthesis, IR spectral, thermal and X-ray single crystal structural analysis of a new mononuclear $[\text{Cd}(\text{bdmpp})(\text{SeCN})_2(\text{H}_2\text{O})]$ complex are presented (Fig. 1).

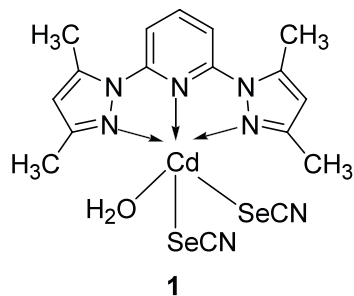


Figure 1. Chemical Structure of $[\text{Cd}(\text{bdmpp})(\text{SeCN})_2(\text{H}_2\text{O})]$ complex (1).

2. Experimental Procedures

2.1. Materials and Measurements

All reagents and solvents were purchased from Merck, Aldrich or Carlo Erba and used without further purification. ^1H - and ^{13}C -NMR spectra were obtained with $\text{DMSO}-d_6$ as solvent and internal TMS as standard using a Bruker AV500 500 MHz spectrometer at room temperature. The elemental analyses for the ligands and complexes were carried out with the Eurovector 3018 CHNS analyzer. Melting points were measured using a Gallenkamp melting point apparatus. IR spectra were obtained by using IR grade KBr discs on a Perkin–Elmer 1600 Series FTIR spectrophotometer in the range of $4000 - 250 \text{ cm}^{-1}$. Electronic spectra were obtained using a Cary 1E UV-Visible Spectrophotometer (Varian). The thermogravimetry/differential thermal analysis (TG/DTA) measurements were run on a Shimadzu DTG-60H instrument. In this study, thermogravimetric curves were obtained with a flow rate of carrier gas at 100 mL min^{-1} and the heating rate of $10 \text{ }^\circ\text{C min}^{-1}$ in nitrogen (3 bar) with the sample contained in an alumina pan. Experiments were carried out in the range $35 - 750^\circ\text{C}$, and the pyrolyzed mixture finally simplified in the range $750 - 800^\circ\text{C}$ under oxygen atmosphere. With the help of the software, TA-60 WS Version 2.01, the data recorded was analyzed.

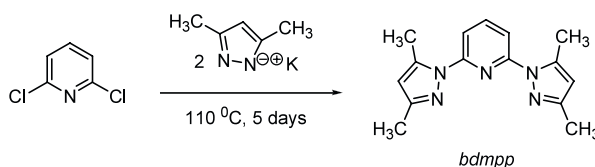
2.2. Preparation of the ligand and the complex

2.2.1. Synthesis of Ligand (bdmpp)

Synthesis of the 2,6-bis(3,5-dimethyl-N-pyrazolyl)pyridine (bdmpp), the bdmpp was performed from 2,6-dichloropyridine and the potassium salt of 3,5-dimethyl-N-pyrazol by refluxing in diglyme [1]. 3,5-Dimethylpyrazol was synthesized by the reaction of hydrazine hydrate and 2,4-pentandione [13].

2.2.2. Synthesis of $[\text{Cd}(\text{bdmpp})(\text{SeCN})_2(\text{H}_2\text{O})]$ (1)

A 20 mL solution of 2,6-bis(3,5-dimethyl-N-pyrazolyl)pyridine (bdmpp) (0,266 g, 1 mmol) in 60°C acetonitrile was added to a 40 mL 60°C methanolic solution of $\text{Cd}(\text{NO}_3)_2 \cdot 4\text{H}_2\text{O}$ (0,308 g, 1 mmol). After mixing well, a 5 mL aqueous solution of KSeCN (0,288 g, 2 mmol) was added (Scheme 1). The mixture was filtered while the solution was at 60°C . The resulting solution was set aside for three or four days and the formed colorless crystals were filtered off and dried in open air. Yield: 67%; ^1H NMR (500 MHz, 25°C , $\text{DMSO}-d_6$), 2.21 (s, 6H), 2.55 (s, 6H), 6.15 (s, 2H), 7.68 (d, 2H, $J = 7.99 \text{ Hz}$), 8.07 (t, 1H, $J = 8.01 \text{ Hz}$); ^{13}C -NMR (125 MHz, 25°C , $\text{DMSO}-d_6$), 13.8, 14.2, 109.6, 114.0, 118.6, 141.0, 141.8, 149.8, 151.3. Anal. Calc. For $\text{C}_{17}\text{H}_{19}\text{CdN}_7\text{OSe}_2$: C, 33,59; H, 3,12; N, 16,13. Found: C, 33,28; H, 3,02; N, 15,87.



Scheme 1. Synthesis of $[\text{Cd}(\text{bdmpp})(\text{SeCN})_2(\text{H}_2\text{O})]$

2.3. Crystal structure determination

Diffraction measurements were made at -100°C on a three-circle CCD diffractometer using graphite monochromated $\text{Mo-K}\alpha$ radiation ($\lambda = 0.71073 \text{ \AA}$) for compound. The intensity data were integrated using the SAINT program [14]. Absorption, Lorentz and polarization corrections were applied. The structures were solved by direct methods and refined using full-matrix least-squares against F^2 using SHELXTL [15–17]. All non-hydrogen atoms were assigned anisotropic displacement parameters and refined without positional constraints. Hydrogen atoms were included in idealized positions with isotropic displacement parameters constrained to 1.5 times the U_{equiv} of their attached carbon atoms for methyl hydrogens, and 1.2 times the U_{equiv} of their attached carbon atoms for all others. The H atoms of the water molecules were located in a

difference Fourier map and refined isotropically. Distance restraints were also applied to the H atoms of the water molecules with a set value of 0.90 (1) Å. The absolute structure was determined on the basis of the Flack [18] parameter $x = 0.014$ (6). The Flack's parameter close to 0 is indicative of a non-centrosymmetric structure. Crystal data collection conditions and parameters of the refinement process of the title compound [Cd(bdmpp)(SeCN)₂(H₂O)] are summarized briefly in Table 1. Crystallographic data (excluding structure factors) for the structure reported in this paper have been deposited with the Cambridge Crystallographic Data Centre as supplementary publication no. CCDC 651075 [19]. Displacement ellipsoids shown in Fig. 2 are plotted at the 50% probability level.

Table 1. Crystal data and structure refinement for the title compound.

Empirical formula	C ₁₇ H ₁₉ CdN ₇ OSe ₂	
Formula weight	607.71	
Temperature	100(2) K	
Wavelength	0.71073 Å	
Crystal system	Monoclinic	
Space group	Cc	
Unit cell dimensions	a = 9.031(2) Å	α = 90°
	b = 13.884(3) Å	β = 100.74(3)°
	c = 16.910(3) Å	γ = 90°
Volume	2083.1(7) Å ³	
Z	4	
Density (calculated)	1.938 g cm ⁻³	
Absorption coefficient	4.566 mm ⁻¹	
F(000)	1176	
θ Range for data collection	2.45 to 27.48°	
Index ranges	-11 ≤ h ≤ 10, -17 ≤ k ≤ 18, -16 ≤ l ≤ 21	
Reflections collected	7253	
Independent reflections	3426 [R(int) = 0.0263]	
Refinement method	Full-matrix least-squares on F ²	
Data / restraints / parameters	3426 / 4 / 263	
Goodness-of-fit on F ²	0.945	
Final R indices [I > 2σ(I)]	R1 = 0.0205, wR2 = 0.0431	
R indices (all data)	R1 = 0.0213, wR2 = 0.0433	
Largest diff. peak and hole	0.912 and -0.866 e Å ⁻³	
Flack parameter	0.014 (6)	

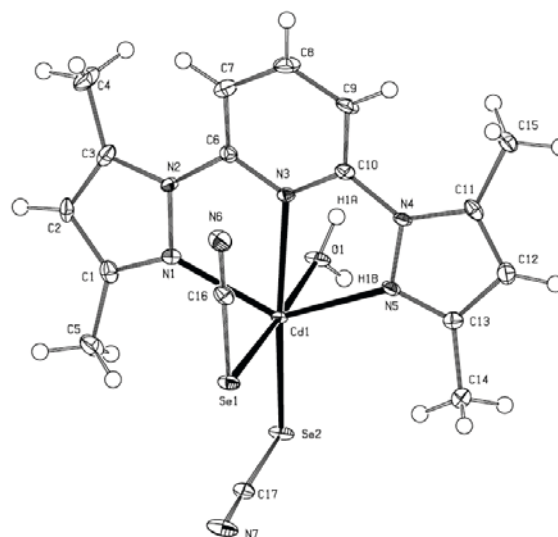


Figure 2. The molecular structure of Cd(bdmpp)(SeCN)₂(H₂O).

2.4. Computational Methods

All calculations reported herein were carried out with the Gaussian 03W program [20] implemented on a high-performance computer. Molecule structures were visualized by using the GaussView program [21]. The geometry of the title complex was optimized separately by using, HF [22] and DFT methods [23] in conjunction with the LANL2DZ basis set [24]. Normal SCF and geometry convergence criteria were used and no symmetry constraints were imposed. Harmonic frequency analysis based on analytical second derivatives was used to characterize the optimized geometry as local minimum on the potential energy surface of complex 1.

3. Results and Discussion

3.1. Description of the crystal structure

The ORTEP and molecular packing diagrams are displayed in Figs. 2, 3 and 4. Some selected bond lengths and angles in the complex are listed in Table 2. Possible hydrogen bonds are also given in Table 3.

The compound (1) crystallizes in the non-centrosymmetric space group Cc but both enantiomers (R and S) are present in the structure, by virtue of the c-glide symmetry. As can be seen from Fig. 2, the molecular structure of Cd(bdmpp)(SeCN)₂(H₂O) has twofold symmetry. The mirror plane dissects the molecule, and the metal atom, the two SeCN and the water molecule are all in the mirror plane. However, chirality of complex (1) is introduced by packing effects. In practical terms: one or more of the ligands that are

normally in the mirror plane are moved out of it. The symmetry is reduced, the mirror planes lost and chirality introduced. It could be that Se1-C16-N6 can be displaced to the left or the right creating two enantiomers. The packing of the title compound **1**, as viewed along the bc plane, is illustrated in Fig. 3. Enantiomers alternate along the c axis. The molecular packing arrangement shows that the two enantiomers self-assemble into homochiral monolayers parallel to the bc plane, respectively, and each monolayer contains just one type of enantiomer. The enantiomeric monolayers are co-packed alternately in the formation of a superlattice with respect to chirality, as shown in Fig. 3. It is noted that the ideal achiral geometry does not exist. The packing pattern shows that the crystal structure is correlated with two real enantiomers rather than with an ideal molecular symmetry [25-27].

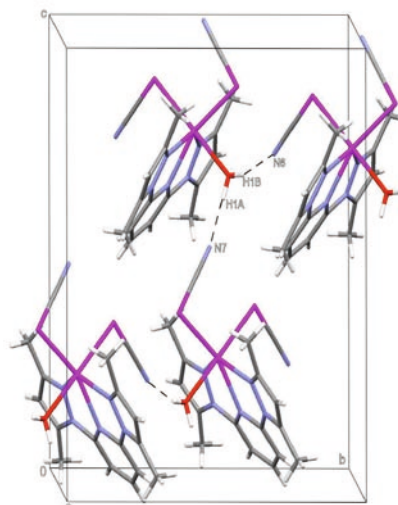


Figure 3. MERCURY view of the packing in the title compound **1**, showing H-bonding motifs in the bc-plane.

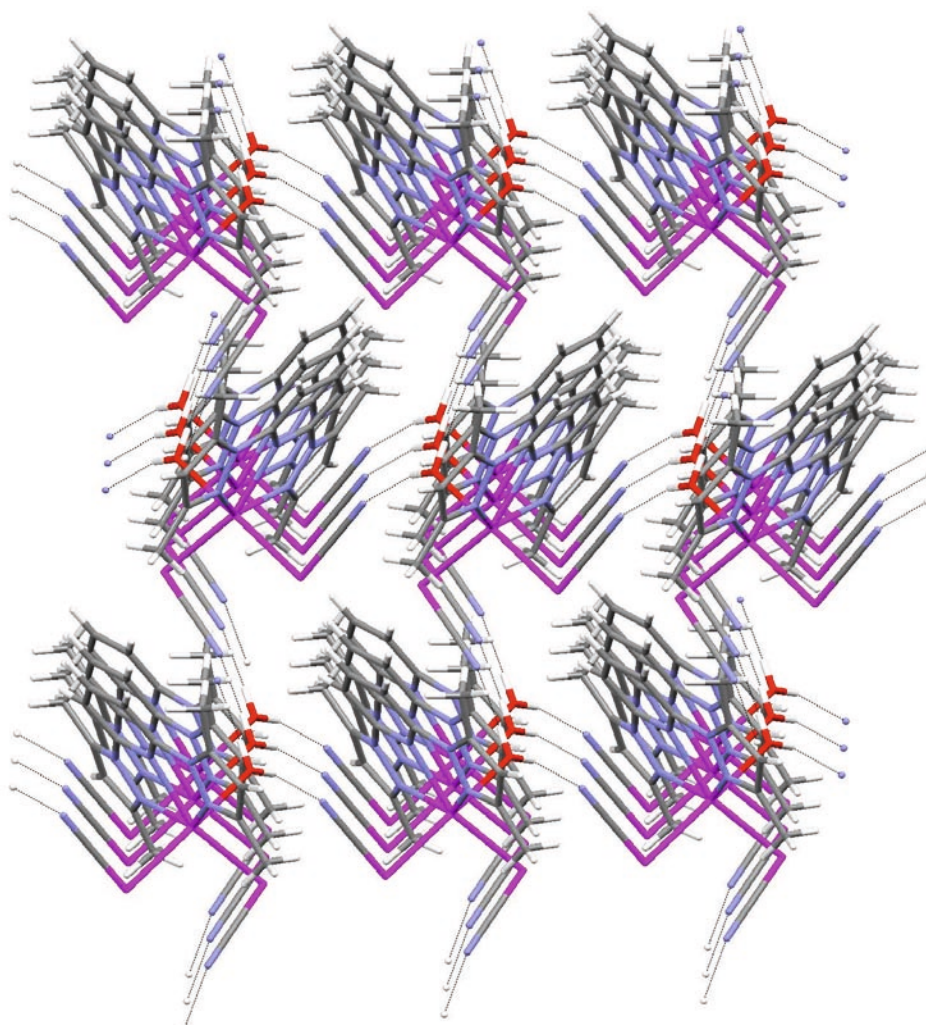


Figure 4. Infinite 3D supramolecular MERCURY view of **1**.

The geometry around the cadmium atom is best described as a distorted octahedron with a CdN₃Se₂O setup. The three nitrogen atoms (N1, N3 and N5) of the 2,6-bis(3,5-dimethyl-N-pyrazolyl) ligand, and a selenium atom (Se2) of the selenocyanate ligand define the equatorial plane around the cadmium atom. The apical positions of the octahedron are occupied by a selenium atom (Se1) of the selenocyanate ligand and the oxygen atom (O1) of the water molecule. Deviation of the cadmium atom from the mean plane formed by the four equatorial atoms is about 0.257 Å. In the coordination network the Cd–N bond distances are in the range 2.336(3) – 2.420(3) Å, the Cd–O1 bond distance is 2.352(3) Å and the Cd–Se1, Cd–Se2 bond distances are 2.753(1), 2.695(1) Å respectively. The selenocyanate groups are quasi-linear as indicated by the Se1–C16–N6 and Se2–C17–N7 angles which

are 179.4(4)° and 178.0(4)°, respectively (Table 2). All the bond lengths and angles are comparable with those in similar structures [3–5]. The N atoms of the SeCN are engaged in two strong intermolecular H-bonding interactions (Table 3, Fig. 3) forming a 3D supramolecular polymeric network (Fig. 4); these H-bonding interactions are responsible for the conformation and stability of the supramolecular polymeric network. This network lies in the bc-plane and stacks orthogonally to the a-axis (Fig. 4). The shortest distances between two Cd(II) centres are 9.031, 8.281 and 8.522 Å in the a, b, c axis directions, respectively.

The geometry of **1** was optimized in singlet and triplet states using the LanL2DZ basis set with the restricted and unrestricted B3LYP functionals, respectively. The energy of the singlet state is of 51.5 kcal mol⁻¹ (including zero-point corrections) lower than that of triplet state.

Table 2. Some selected bond lengths [Å] and bond angles [°] for the title compound.

	X-ray	DFT methods with LanL2DZ basis set				
		Ab-initio method RHF/LanL2DZ	BLYP	B3LYP	B3PW91	MPW1PW91
<i>Bond lengths</i>						
Cd(1)–N(1)	2.336	2.410	2.425	2.401	2.388	2.378
Cd(1)–N(3)	2.420	2.418	2.446	2.418	2.398	2.391
Cd(1)–O(1)	2.352	2.468	2.419	2.398	2.393	2.384
Cd(1)–Se(1)	2.753	2.796	2.889	2.849	2.820	2.807
N(1)–N(2)	1.382	1.388	1.430	1.408	1.398	1.394
C(1)–N(1)	1.326	1.317	1.362	1.346	1.344	1.341
C(6)–N(2)	1.418	1.407	1.435	1.422	1.416	1.413
C(6)–N(3)	1.325	1.329	1.364	1.349	1.345	1.342
C(10)–N(4)	1.406	1.405	1.429	1.417	1.412	1.409
C(16)–N(6)	1.144	1.161	1.208	1.193	1.192	1.189
C(16)–Se(1)	1.830	1.875	1.872	1.863	1.856	1.853
<i>R²</i>	-	0,997	0,997	0,998	0,998	0,998
<i>Bond Angles</i>						
N(1)–Cd(1)–O(1)	87.70	84.62	87.50	86.78	86.82	86.64
N(1)–Cd(1)–N(5)	134.25	134.90	134.34	134.74	135.35	135.40
N(1)–Cd(1)–N(3)	67.15	68.08	68.07	68.18	68.35	68.42
N(1)–Cd(1)–Se(1)	89.89	98.77	98.33	98.37	98.24	98.51
N(1)–Cd(1)–Se(2)	110.48	109.57	110.70	110.07	109.92	109.71
O(1)–Cd(1)–N(5)	86.70	84.62	87.50	86.78	86.82	86.64
O(1)–Cd(1)–Se(1)	177.59	170.27	170.25	170.79	171.08	170.81
N(3)–Cd(1)–Se(1)	100.94	94.66	92.58	92.40	92.63	92.56
N(5)–Cd(1)–Se(2)	113.85	110.78	111.63	111.69	111.56	111.58
Se(2)–Cd(1)–Se(1)	97.52	98.83	94.31	95.30	95.07	95.35
C(1)–N(1)–Cd(1)	134.4	134.61	136.52	136.02	135.78	135.65
<i>R²</i>	-	0,981	0,979	0,980	0,980	0,979

Table 3. Hydrogen-bond geometry (Å) for the title compound.

D–H ... A	D–H	H...A	D...A	D–H...A
O1–H1A ... N7 ⁱ	0.87 (3)	1.94 (3)	2.812 (4)	173 (4)
O1–H1B ... N6 ⁱⁱ	0.89 (3)	1.95 (3)	2.802 (4)	159 (3)

Symmetry codes: (i) [x, -y+1, z-1/2], (ii) [x+1/2, y-1/2, z]

The optimized geometric parameters of the singlet state obtained from HF and DFT calculations are gathered in Table 2. In general, the predicted bond lengths and angles at both *ab-initio* and DFT levels are in good agreement with the values based upon the X-ray crystal structure data of **1** whereas, the results of bond angles obtained by B3LYP and B3PW91 methods are better than those obtained by others. Moreover, some differences may be noticed between the experimental and calculated structures. It may result from the computational methods which are approximated to a certain extent or may indicate the influence of the crystal packing, especially strong intermolecular H-bonding interactions, on the values of the experimental bond lengths and angles. The computational calculations presented here do not consider the effects of chemical environment on complex **1**.

3.2. FTIR Spectra

The IR spectra of $[\text{Cd}(\text{bdmpp})(\text{SeCN})_2(\text{H}_2\text{O})]$ in KBr pellets show absorption bands due to $\nu_{\text{C=N}}$ of the monodentate SeCN⁻ ion around 2105 and 2115 cm^{-1} , and $\nu_{\text{C-Se}}$ lies at about 566 cm^{-1} (Se-Cd bonding) [28]. The FTIR spectrum of the free ligand shows weak peaks at 2977, 2921 cm^{-1} and 3134, 3106 cm^{-1} , assignable to CH_3 and aromatic hydrogen bonds, respectively. The band at 1590 cm^{-1} in the free ligand shifts to 1615 cm^{-1} showing that there is a non-coordinated pyridine ring. The FTIR spectra of the title complex clearly show the characteristic medium and broad absorptions in the 3340 cm^{-1} region due to ν_{OH} stretch of the coordinated water. The regression analyses (R^2) of experimental

and calculated wave numbers with *ab-initio* and DFT methods were also presented in Table 4. It can be seen that R^2 values obtained for DFT methods (BLYP, B3LYP, B3PW91, and MPW1PW91) are better than that for *ab-initio* method (RHF/LanL2DZ). DFT accounting for electron correlation effects may be one of the reasons for the better performance of this method *versus* HF. Moreover, the experimental vibrational frequencies are especially in better agreement with B3LYP results than with other DFT results given in Table 4.

3.3. Absorption spectra

The absorption spectra of the ligand (bdmpp) and complex $[\text{Cd}(\text{bdmpp})(\text{SeCN})_2(\text{H}_2\text{O})]$ were recorded in dimethylformamide, because the complex only has reasonable solubility in this solvent. The UV spectra for ligand and complex show two strong absorptions bands between 250 and 310 nm. For the bdmpp complex, a band occurs near 266 nm (ϵ_1 , 17130 $\text{M}^{-1} \text{cm}^{-1}$) with a shoulder at 298 nm (ϵ_2 , 18790 $\text{M}^{-1} \text{cm}^{-1}$). The spectra of the free ligand exhibit intense peaks at 258 (12 800 $\text{M}^{-1} \text{cm}^{-1}$) and 300 nm, indicating that ligand-centered bands occur in this region, although other charge-transfer transitions also may contribute significant intensity. The relative intensity of this band (300 nm) was lower than that in the free ligand. A similar observation was mentioned by Willison *et al.* [29]. For comparison, coordination of 2,2'-bipyridine to an acidic metal center is known to result in intense and structured $\pi-\pi^*$ absorption in the vicinity of 290 - 310 nm that is very different from the spectrum of the free ligand [30].

Table 4. Observed and Calculated Vibrational Frequencies of Complex 1.

Observed freq.	Ab-initio method		DFT methods with LanL2DZ basis set		
	RHF/LanL2DZ	BLYP	B3LYP	B3PW91	MPW1PW91
3334	3994	3319	3533	3556	3570
3135	3229	3138	3128	3180	3166
3108	3220	3077	3125	3064	3076
2116	2386	2010	2116	2129	2152
2106	2385	1992	2104	2116	2141
1606	1601	1568	1603	1621	1634
1563	1536	1561	1531	1541	1555
1469	1497	1441	1456	1468	1480
1383	1420	1384	1384	1403	1390
1307	1268	1323	1312	1341	1354
1136	1112	1115	1121	1146	1178
1043	1086	1053	1060	1065	1034
985	949	976	912	1017	873
826	803	829	824	829	837
784	749	782	769	758	764
736	717	715	741	752	758
657	606	693	654	659	657
R^2	0.985	0.988	0.997	0.996	0.995

The selected HOMO and LUMO orbitals of complex **1** and their energies computed at B3LYP/LanL2DZ level are depicted in Fig. 5. HOMO-1 and HOMO orbitals are substantially localized on the SeCN part of complex, especially the π -bonding orbitals of Se atoms. On the contrary, the LUMO orbital is mainly confined in the aromatic part of the complex and the LUMO + 1 orbital is widely localized on the π -antibonding orbitals of the cadmium atom. Moreover, the frontier molecular orbital energies play an important role in the electric and optical properties, as well as in UV-Vis spectra and chemical reactions in the conjugated molecules [31]. The HOMO-LUMO energy gap is 0.129 eV, allowing electron movement between these orbitals to easily occur so that a peak around 250 - 310 nm can be observed in the UV-Vis spectrum.

3.4. NMR data of bdmpp and 1

The $^1\text{H-NMR}$ and $^{13}\text{C-NMR}$ spectra of the complex show the expected integration and peak multiplicities, indicating that substitution of water and selenocyanate ligands takes place without significant changes in the geometry of the free ligand (*bdmpp*). The chemical shifts of the signal for the protons of methyl groups (2.21 and 2.55 ppm), the protons of pyrazole groups (6.15 ppm), the protons of the pyridine group (7.68 and 8.07 ppm) appear at almost the same position as in the free ligand. In $^{13}\text{C-NMR}$ spectra, the resonance at 118.6 ppm is attributed to the carbon atoms of selenocyanate groups, participating in coordination to Cd(II).

3.5. Thermal behaviour

The TGA and DTA analysis of the complex (**1**) was investigated both under inert and open-air atmosphere. As the results obtained from the TGA-DTA thermogram of (**1**) show, there is no changing up to 210°C. The complex starts to melt at 220°C on the DTA plot. It is observed that during the melting the complex also starts to decompose. The DTA melting peak is seen clearly because there is no complete decomposition. Between 230 - 410°C, it can be conceived that the 55% mass

loss with a large thermal decomposition belongs to the bdmpp ligand because the ratio of the bdmpp ligand in the complex is 53.93%. The probability is that the ligand is separated gradually. It is possible to see the steps of the decomposition between 230 - 410°C. There is only one DTA peak at 289°C that belongs to the situation. Above 410°C the $\text{Cd}(\text{SeCN})_2$ in the medium slowly turns to CdSe and there exists the pyrolysis product and carbon that remains from the decomposition of the organic ligand. At 800°C when O_2 is introduced this carbon residue and CdSe form CdO by burning, and at this temperature only the CdO remains.

4. Conclusion

The mononuclear distorted octahedral Cd(II) complex with bdmpp and selenocyanate has been synthesized and investigated using elemental analyses, infrared and electronic spectra, $^1\text{H-}$ and $^{13}\text{C-NMR}$ spectra, X-ray diffraction and thermal analysis. Even though the selenocyanate ion tends to form μ -bridges which result in the formation of polynuclear complexes [32], the selenocyanate ion here is connected as a terminal ion. Hence, a mononuclear Cd(II) complex was obtained. From the calculations, the experimental IR frequencies of complex **1** are especially in better agreement with B3LYP/LanL2DZ results than those from other methods.

Acknowledgements

The financial support of the Scientific and Technical Research Council of Turkey (TUBITAK) Grants No: TBAG-104T064, TBAG-104T371 and TBAG-108T431, and Balikesir University is gratefully acknowledged. Hulya Kara also thanks the Nato-B1-TUBITAK for funding and Prof. Guy Orpen (School of Chemistry, University of Bristol, UK) for his hospitality. We are also grateful to one of reviewers for helpful suggestions.

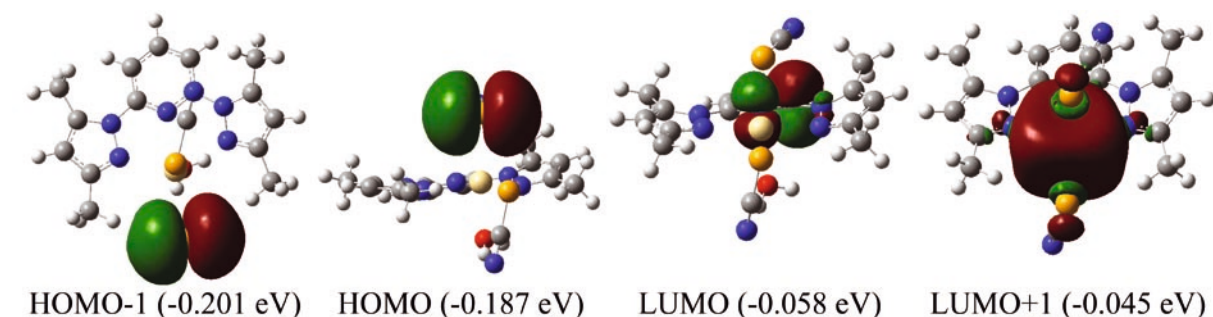


Figure 5. The calculated HOMO and LUMO orbitals and their energies at B3LYP/LanL2DZ level.

References

- [1] L. Jameson, K.A. Goldsby, *J. Org. Chem.* 55, 4992 (1990)
- [2] R. Kurtaran, H. Namli, C. Kazak, O. Turhan, O. Atakol, *J. Coord. Chem.* 60, 2133 (2007)
- [3] C. Arıcı, D. Ülkü, R. Kurtaran, K.C. Emregül, O. Atakol, *Z. Kristallogr.* 218, 497 (2003)
- [4] R. Kurtaran, S. Odabasioglu, A. Azizoglu, H. Kara, O. Atakol, *Polyhedron* 26, 5069 (2007)
- [5] R. Kurtaran, C. Arıcı, K.C. Emregül, D. Ülkü, O. Atakol, M. Tastekin, *Z. Anorg. Allg. Chem.* 629, 1617 (2003)
- [6] F. Ercan, C. Arıcı, D. Ülkü, R. Kurtaran, M. Aksu, O. Atakol, *Z. Kristallogr.* 219, 295 (2004)
- [7] C. Diaz, J. Ribas, N. Sanz, X. Solans, M.C. Bardia, *Inorg. Chim. Acta* 286, 169 (1999)
- [8] a) A. Escuer, R. Vicente, F.A. Mautner, M.A.S. Goher, *Inorg. Chem.* 36, 1233 (1997); b) H-P. Jia, W. Li, Z-F Ju, J. Zhang, *Inorg. Chem. Commun.* 10, 397 (2007)
- [9] a) L. Pazderski, A. Surdykowski, M. Pazderska-Szablowicz et al., *Cent. Eur. J. Chem.* 6, 55 (2008); b) H.R. Khavasi, A. Abedi, V. Amani et al., *Polyhedron* 27, 1848 (2008); c) M.D. Brown, J.M. Dyke, F.Ferrante, W. Levason, J.S. Ogden, M. Webster, *Chem. Eur. J.* 12, 2620 (2006)
- [10] a) H. Grove, M. Julve, F. Lloret, P.E. Kruger, K.W. Törnroos, J. Sletten, *Inorg. Chim. Acta* 325, 115 (2001) b) A.V. Chekhlov, *J. Struct. Chem.* 44, 335 (2003)
- [11] C.R. Choudhury, S.K. Dey, N. Mondal, S. Mitra, V. Gramlich, *Inorg. Chim. Acta* 353, 217 (2003)
- [12] T.K. Maji, G. Mostafa, P.S. Mukherjee, A. Mondal, A.J. Welch, K. Okamoto, N.R. Chaudhuri, *Polyhedron* 19, 1903 (2000)
- [13] B.S. Furniss, A.J. Hannaford, P.W.G. Smith, A.R. Tatchell, *Vogel's Textbook of Practical Organic Chemistry*, 5th Edition (Longman, Scientific and Technical, London, 1989) 1149
- [14] SAINT integration software version 7.06A (Bruker AXS, Madison, WI, 1997-2003)
- [15] SHELXTL program system version 6.14 (Bruker AXS Inc., Madison, WI, 2000-2003)
- [16] SMART diffractometer control software version 5.628(APEX) (Bruker AXS Inc., Madison, WI, 1997-2002)
- [17] G.M. Sheldrick, *SADABS* version 2.05 (University of Göttingen, Germany, 2003)
- [18] H.D. Flack, *Acta Cryst.* A39, 876 (1983)
- [19] CCDC-651075 contains the supplementary crystallographic data for this paper. These data can be obtained free of charge via www.ccdc.cam.ac.uk/data_request/cif, or by emailing data_request@ccdc.cam.ac.uk, or by contacting The Cambridge Crystallographic Data Centre, 12, Union Road, Cambridge CB2 1EZ, UK; fax: +44 1223 336033
- [20] M.J. Frisch et al., *Gaussian 03*, Revision C02 (Gaussian Inc., Pittsburgh PA, 2003)
- [21] R. Dennington II, T. Keith, J. Millam, K. Eppinnett, W.L. Hovell, R. Gilliland, *GaussView*, Version 3.09 (Semichem, Inc., Shawnee Mission, KS, 2003)
- [22] W.J. Hehre, L. Radom, P.V. Schleyer, J. Pople, *Ab initio molecular orbital theory* (Wiley, New York, 1986)
- [23] F. Jensen, *Introduction to computational chemistry* (Wiley, UK, 1999)
- [24] P.J. Hay, W.R. Wadt, *J. Chem. Phys.* 82, 299 (1985)
- [25] J.D. Dunitz, *Chem. Commun.* 545 (2003)
- [26] E. Pidcock, W.D.S. Motherwell, *Cryst. Growth & Des.* 4, 611 (2004)
- [27] D.W.M. Hofmann, L.N. Kuleshova, M.Y. Antipin, *Cryst. Growth & Des.* 4, 1395 (2004)
- [28] S-L. Li, J-Y. Wu, Y-P. Tian, H. Ming, P. Wang, M-H. Jiang, K-K. Fun, *Eur. J. Inorg. Chem.* 2900 (2006)
- [29] S.A. Willison, H. Jude, R.M. Antonelli, J.M. Rennekamp, N.A. Eckert, A. Jeanette, B. Krause, W.B. Connick, *Inorg. Chem.* 43, 2548 (2004)
- [30] (a) R.G. Bray, J. Ferguson, C.J. Hawkins, *Aust. J. Chem.* 22, 2091 (1969); (b) T. Ohno, S. Kato, *Bull. Chem. Soc. Jpn.* 47, 2953 (1974)
- [31] a) I. Fleming, *Frontier Orbitals and Organic Chemical Reactions* (Wiley, London, 1976); b) L. Turker, A. Azizoglu, *J. Mol. Struct. (THEOCHEM)* 535, 151 (2001); c) A. Azizoglu, *Struct. Chem.* 14, 575 (2003); d) A. Viridi, V.P. Gupta, A. Sharma, *Cent. Eur. J. Chem.* 2, 456 (2004); e) B.B. Koleva, T. Kolev, R. Nikolova, Y. Zagraniansky, M. Spittler, *Cent. Eur. J. Chem.* 6, 592 (2008)
- [32] Q.M. Wang, G.C. Guo, T.C.W. Mak, *Polyhedron* 20, 2683 (2001); b) M. Broering, S. Prikhodovski, E.C. Tejero, S. Koehler, *Eur. J. Inorg. Chem.* 1010 (2007)